

## Journal of Applied and Theoretical Physics Research

### Lifshitz Transition in Topological Insulators with Second and Third-Neighbor Interactions

José Solano de Morais Neto<sup>1</sup> and Anilton de Brito Vieira Filho<sup>2\*</sup>

<sup>1</sup>Instituto de Física, Universidade Federal de Brasília, Brasília

<sup>2</sup>Departamento de Física, Universidade Federal do Ceará, Ceará

**\*Corresponding author:** Anilton de Brito Vieira Filho, Departamento de Física, Universidade Federal do Ceará, Caixa Postal 6030, Campus do Pici, 60455-760 Fortaleza, Ceará, Brazil; E mail: anilton@fisica.ufc.br

**Article Type:** Research, **Submission Date:** 02 August 2017, **Accepted Date:** 31 August 2017, **Published Date:** 14 November 2017.

**Citation:** José Solano de Morais Neto and Anilton de Brito Vieira Filho (2017) Lifshitz Transition in Topological Insulators with Second and Third-Neighbor Interactions. J Apl Theol 1(3): 1-5.

**Copyright:** © 2017 José Solano de Morais Neto and Anilton de Brito Vieira Filho. This is an open-access article distributed under the terms of the Creative Commons Attribution License, which permits unrestricted use, distribution, and reproduction in any medium, provided the original author and source are credited.

Topological Lifshitz transitions involve many types of topological structures in momentum and frequency-momentum spaces, where the energy band of a topological insulator is calculated taken into account second and third neighbors. A tight-binding model based on the Bernevig-Hughes Zhang (BHZ) approach for quantum wells is used to calculate the energies. The BHZ is characterized by the mass term  $M(k) = \Delta - Bk^2$ . In the microscopic theory used here, the mass term is  $M(k) = \Delta - 2B(2 - \cos(k_x a) - \cos(k_y a))$  that is modified when second and/or third neighbors are included in the model, as a consequence the range where the material is an insulator is changed.

#### Introduction

The key word in consideration of Lifshitz transitions is topology. Following original Lifshitz paper [1], Lifshitz transition has been viewed as a change of the topology of the Fermi surface without symmetry breaking. The combination of topology of the shape of the Fermi surfaces, Fermi lines and Fermi points together with the topology, which supports the stability of these objects, and also the topology of the interconnections of the objects of different dimensions provide a large number of different types of Lifshitz transitions (some of the are discussed in Refs.[2,3]). This makes the Lifshitz transitions ubiquitous with applications to high energy physics, cosmology, black hole physics and to search for the room-T superconductivity.

The topological insulators (TIs) were first predicted in graphene where spin-orbit interactions were included [4,5]. The quantum spin hall effect generates an energy gap in the bulk system. However, the system has edge helicoidal gapless states with spins moving in opposite directions, with little or no dissipation, which are topologically protected against moderate electronic interactions or nonmagnetic disorder. The edge states are

massless Dirac Fermions that cross the whole forbidden gap separating the valence and conduction band. By helicity of edge states we mean that electrons with the same spin can move only in one direction, which is opposite for two spin directions. As a result, the edge states are robust against elastic backscattering, which conserves spin, and the electron transport along edges becomes ballistic, that turn these materials into promising ones for many applications, such as spintronics and quantum devices. These Dirac-like states are protected by time-reversal symmetry (TRS)[6] or by crystal symmetry [7-9].

Understanding the properties of the edge states has been an interesting aspect of TIs theoretical studies [10-14]. It can be done by constructing an appropriate tight binding model Hamiltonian and examining their eigenstates for lattices with boundaries. A very useful model was proposed by Benevig, Hugues e Zhang (BHZ) that is based on HgTe/CdTe quantum wells (QWs). The crucial ingredient of this narrow gap semiconductor structure is the inverted band structure of HgTe. In the HgTe/CdTe QWs, the topological phase is determined by the sign of the Dirac mass  $M$ . The gap between the E1 (s-like) and the H1 (p-like) subbands at the  $\Gamma$  point is given by  $2|M|$ . The only experimentally accessible parameter tuning the Dirac mass from normal ( $M > 0$ ) to inverted ( $M < 0$ ) is the thickness of the HgTe QW. In particular, a topological transition from the normal to the topological insulating phase takes place when the QW thickness is increased above the critical thickness  $d_c = 6.3\text{nm}$ . Bernevig et al [15] predicted samples with such an inverted band structure to be quantum spin Hall insulators with a band gap of tens of meV, which was soon verified experimentally [16]. A peculiar feature in the electronic structure of these states is the existence of so called Lifshitz points, where the change in topology of constant energy contours occurs. By varying the filling of the surface

states, the Lifshitz transitions could, in principle, be induced, with interesting consequences on surface transport.

### Tight-Binding Hamiltonian for $Z_2$ Topological Insulators

The model used to describe the  $Z_2$  topological insulators is constituted by a square lattice, where each site on the network contains two orbitals, where one has odd and the other even parity. The orbital with odd parity has a higher energy than the orbital with even parity. This model is a simplification of the Bernevig-Hughes-Zhang model for quantum wells that have recently attracted much attention in the study of two-dimensional topological insulators with protected helicoidal states of edge.

The Tight-Binding Hamiltonian is given by,

$$H_{\uparrow} = \sum_{i,\sigma} \delta^{\sigma} a_{i,\sigma}^{\dagger} a_{i,\sigma} - \frac{1}{2} \sum_{i,j,\sigma,\sigma'} (t_{ij}^{\sigma\sigma'} a_{i,\sigma}^{\dagger} a_{j,\sigma'} + hc) \quad (1)$$

where  $i, j$  runs over all sites of the lattice,  $a_{i,\sigma}^{\dagger}$  ( $a_{i,\sigma}$ ) creates (annihilates) an electron on site  $i$

in orbital  $\sigma$ .  $\sigma$  and  $\sigma'$  stand for  $s$  or  $p$ ,  $t^{ss(pp)}$  is a constant defining the hopping in the same orbital. Here  $t_1$  is the nearest neighbor coupling between different orbitals. The  $t^{ss}$  and  $t^{pp}$  are constants, and the  $t^{sp} = \exp(i\theta_{ij})t_1$  ( $t^{ps} = \exp(-i\theta_{ij})t_1$ ) depends on the lattice orientation and  $\theta_{ij}$  is the angle of the wavevector propagation in the lattice. The Hamiltonian can now be rewritten in the plane wave orbital basis

$$H_k = \sum_k \left[ \dot{\delta}_0^{(s)} - 2t_s (\cos(k_x a) + \cos(k_y a)) \right] a_{k,s}^{\dagger} a_{k,s} - 2it_1 \left[ \sin(k_x a) + i \sin(k_y a) \right] a_{k,s}^{\dagger} a_{k,p} + \left[ \dot{\delta}_0^{(p)} - 2t_p (\cos(k_x a) + \cos(k_y a)) \right] a_{k,p}^{\dagger} a_{k,p} - 2it_1^* \left[ -\sin(k_x a) + i \sin(k_y a) \right] a_{k,p}^{\dagger} a_{k,s} \quad (2)$$

and the Hamiltonian can be written as

$$H_k = \sum_k \left[ \dot{\delta}(k) + \Delta - 2B(2 - \cos(k_x a) - \cos(k_y a)) \right] a_{k,s}^{\dagger} a_{k,s} + A \left[ \sin(k_x a) + i \sin(k_y a) \right] a_{k,s}^{\dagger} a_{k,p} \left[ \dot{\delta}(k) - \Delta + 2B(2 - \cos(k_x a) - \cos(k_y a)) \right] a_{k,p}^{\dagger} a_{k,p} - A^* \left[ -\sin(k_x a) + i \sin(k_y a) \right] a_{k,p}^{\dagger} a_{k,s} \quad (3)$$

where

$$t_p - t_s = B$$

$$\dot{\delta}_0^{(s)} - \dot{\delta}_0^{(p)} + 4t_p - 4t_s = 2\Delta,$$

$$A = 2it_1,$$

$$\dot{\delta}(k) = \frac{\dot{\delta}_0^{(s)} - \dot{\delta}_0^{(p)}}{2} - (t_s + t_p) [\cos(k_x a) + \cos(k_y a)]. \quad (7)$$

giving the energies

$$E = \sqrt{(A(k))^2 + (M(k))^2}, \quad (8)$$

with  $(A(k))^2 = A^2 (\sin^2(k_x a) + \sin^2(k_y a))$  and  $M(k) = \Delta - 2B(2 - \cos(k_x a) - \cos(k_y a))$ .

The Table 1 below shows the parameters combination that give a zero gap in the energy band. The gap closes in  $\Gamma$  point for  $\Delta = 0$ ,  $X_1$  and  $X_2$  when  $\Delta = 4B$ , while closes in  $M$  when  $\Delta = 8B$ . There are topological quantum phase transition in these points.

**Table 1:** The combinations of wave-vector and  $M$  resulting in a gapless spectra with the respective Brillouin zone point

BZ	$k_x$	$k_y$	$\Delta$
$\Gamma$	0	0	0
$X1$	0	$\pi$	$4B$
$X2$	$\pi$	0	$4B$
$M$	$\pi$	$\pi$	$8B$

A topological insulator exists when the parameters  $\Delta$  and  $B$  fall in the range,  $0 < \Delta/B < 4$  or  $4 < \Delta/B < 8$ . At  $\Delta/B = 4$ , which separates the cases of positive and negative quantized spin Hall conductivities. The equation (1) shows the dispersion relation for the topological insulator. The energy increases with increasing the value of the parameters  $A_1$  and  $B_1$ .  $A_1$  and  $B_1$  parameter does not change the gap, it shifts the energy everywhere but the  $\Gamma$  point [17].

### Tight-Binding Hamiltonian for $Z_2$ Topological Insulators with Interaction between Nearest-, Second-, and Third-Neighbor

Next, we consider the tight-binding Hamiltonian with interaction between nearest-, second-, and third-neighbor on a square lattice (see Figure 1). The hamiltonian has the same forma as in the previous case, what changes is the structure factos to include the new interactions.

$$H_k = \sum_k \left[ \dot{\delta}_0^{(s)} - 2t_s (\cos(k_x a) + \cos(k_y a)) - 4t_s^{(2)} (\cos(k_x a) \cos(k_y a)) - 2t_s^{(3)} (\cos(2k_x a) + \cos(2k_y a)) \right] a_{k,s}^{\dagger} a_{k,s} + (A_1(k) + A_2(k) + A_3(k)) a_{k,s}^{\dagger} a_{k,p} + (A_1^*(k) + A_2^*(k) + A_3^*(k)) a_{k,p}^{\dagger} a_{k,s} + \left[ \dot{\delta}_0^{(p)} - 2t_p (\cos(k_x a) + \cos(k_y a)) - 4t_p^{(2)} (\cos(k_x a) \cos(k_y a)) - 2t_p^{(3)} (\cos(2k_x a) + \cos(2k_y a)) \right] a_{k,p}^{\dagger} a_{k,p}, \quad (9)$$

(5) where  $A_1(k) = 2it_1 [\sin(k_x a) + i \sin(k_y a)]$ ,  $A_2(k) = 2i(2)^{1/2} t_2 (\sin(k_x a) \cos(k_y a) + i \sin(k_y a) \cos(k_x a))$  and  $A_3(k) = 2it_3 [\sin(k_x a) + i \sin(k_y a)]$ . The Hamiltonian can be written as

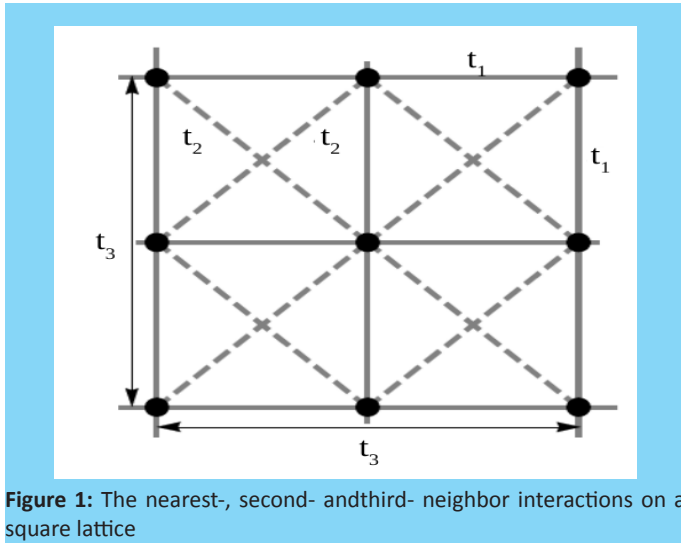


Figure 1: The nearest-, second- and third- neighbor interactions on a square lattice

$$\begin{aligned}
 H_k = & \sum_k \begin{bmatrix} \hat{\sigma}(k) + \Delta - 2B(2 - \cos(k_x a) - \cos(k_y a)) \\ -2B_2(2 - 2\cos(k_x a)\cos(k_y a)) \end{bmatrix} a_{k,s}^\dagger a_{k,s} \\
 & - \begin{bmatrix} 2B_3(2 - \cos(2k_x a) - \cos(2k_y a)) \end{bmatrix} a_{k,s}^\dagger a_{k,s} \\
 & + \begin{bmatrix} A \begin{pmatrix} \sin(k_x a) \\ +i\sin(k_y a) \end{pmatrix} + A_3(\sin(2k_x a) + i\sin(2k_y a)) \\ A_2\sqrt{2}(\sin(k_x a)\cos(k_y a) + i\sin(k_y a)\cos(k_x a)) \end{bmatrix} a_{k,s}^\dagger a_{k,p} \\
 & + \begin{bmatrix} \hat{\sigma}(k) - \Delta + 2B(2 - \cos(k_x a) - \cos(k_y a)) \\ +2B_2(2 - 2\cos(k_x a)\cos(k_y a)) \end{bmatrix} a_{k,p}^\dagger a_{k,p} \\
 & + 2B_3(2 - \cos(2k_x a) - \cos(2k_y a)) a_{k,p}^\dagger a_{k,p} \\
 & + \begin{bmatrix} -A^* \begin{pmatrix} -\sin(k_x a) \\ +i\sin(k_y a) \end{pmatrix} - A_3^* \begin{pmatrix} -\sin(2k_x a) \\ +i\sin(2k_y a) \end{pmatrix} \\ -A_2^*\sqrt{2}(-\sin(k_x a)\cos(k_y a) + i\sin(k_y a)\cos(k_x a)) \end{bmatrix} a_{k,p}^\dagger a_{k,s} \\
 & + \begin{bmatrix} -A_2^*\sqrt{2}(-\sin(k_x a)\cos(k_y a) + i\sin(k_y a)\cos(k_x a)) \end{bmatrix} a_{k,p}^\dagger a_{k,s}
 \end{aligned}$$

where

$$t_p - t_s = 2B, t_p^{(2)} - t_s^{(2)} = 2B_2, t_p^{(3)} - t_s^{(3)} = 2B_3, \quad (11)$$

$$\hat{\sigma}_0^{(s)} - \hat{\sigma}_0^{(p)} + 4t_p - 4t_s + 4t_p^{(2)} - 4t_s^{(2)} + 4t_p^{(3)} - 4t_s^{(3)} = 2\Delta, \quad (12)$$

$$A = 2it_1, A_2 = 2it_2, A_3 = 2it_3, \quad (13)$$

$$\begin{aligned}
 \hat{\sigma}(k) = & \frac{\hat{\sigma}_0^{(s)} - \hat{\sigma}_0^{(p)}}{2} - (t_s + t_p)(\cos(k_x a) + \cos(k_y a)) \\
 & - 2(t_s^{(2)} + t_p^{(2)})(\cos(k_x a)\cos(k_y a)) - (t_s^{(3)} + t_p^{(3)})(\cos(k_x a) + \cos(k_y a)),
 \end{aligned} \quad (14)$$

giving the energies

$$E = \sqrt{\Omega^2 + (\Delta - D)^2}, \quad (15)$$

with  $D = 2B(2 - \cos(k_x a) - \cos(k_y a)) + 2B_2(2 - 2\cos(k_x a)\cos(k_y a)) + 2B_3(2 - \cos(2k_x a) - \cos(2k_y a))$  and

$$\begin{aligned}
 \Omega^2 = & A^2(\sin^2(k_x a) + \sin^2(k_y a)) + 2AA_2 \begin{pmatrix} \sin^2(k_x a)\cos(k_y a) \\ +\sin^2(k_y a)\cos(k_x a) \end{pmatrix} \\
 & + A_3^2(\sin^2(2k_x a) + \sin^2(2k_y a)) + 2AA_3 \begin{pmatrix} \sin(k_x a)\sin(2k_x a) \\ +\sin(k_y a)\sin(2k_y a) \end{pmatrix} \\
 & + A_2^2(\sin^2(k_x a)\cos^2(k_y a) + \sin^2(k_y a)\cos^2(k_x a)) \\
 & 2A_2A_3(\sin(2k_x a)\sin(k_x a)\cos(k_y a) + \sin(2k_y a)\sin(k_y a)\cos(k_x a)).
 \end{aligned} \quad (16)$$

As in the case for next-neighbor the spectra becomes gapless for the parameters show in Table 2.

**Table 2:** The combinations of wave-vector and  $\Delta$  resulting in a gapless spectra with the respective Brillouin zone points. Now considering second- and third-neighbors

BZ	$k_x$	$k_y$	$\Delta$
$\Gamma$	0	0	$-4(B_2 + B_3)$
$X1$	0	$\pi$	$4(B + B_2 - B_3)$
$X2$	$\pi$	0	$4(B + B_2 - B_3)$
$M$	$\pi$	$\pi$	$8B - 4(B_2 + B_3)$

The new transitions occurs for  $\Delta = -4(B_2 + B_3)$ ,  $\Delta = 4(B + B_2 - B_3)$ , and  $\Delta = 8B - 4(B_2 + B_3)$ .

### Lifshitz Transition in Topological Insulator

In Figure 2 the dispersion relation for the topological insulator is shown in a contour plot for four different values of the inter-orbital hopping. The energy increases from blue to red. As we have chosen  $\Delta = 2.0$ ,  $A_1 = 1.0$ ,  $B_1 = 1.0$ ,  $A_2 = 0.2$ ,  $B_2 = 0.2$  and  $B_3 = 0.04$ , the gap closes only for the  $\Gamma$  point. The increase in the  $A_3$  parameter does not change the gap, it shifts the energy everywhere but the  $\Gamma$  point. In Figure 3 the  $A_3$  parameter is fixed to show the contour plot for different values of the parameter  $B_3$  and  $\Delta = 2.0$ . For  $B_3 = 0$  the gap closes for point  $\Gamma$ . The energies increases with  $B_3$  (from blue to red) but in a different way of Figure 1. In Figure 4 we fixed the hopping parameters and changed  $\Delta$  to show the energy contour plot of the dispersion relation. The band energy changes significantly as we increase  $\Delta$  and the zero gap depends on the hopping parameters. As compared with the first neighbors case, the one with second and third neighbors gives much more possibilities for the zero gap to exist. We can also note a Lifshitz transition along  $X_1 - \Gamma - X_2$ . Due to the effect of second and third neighbors on the topological insulator.

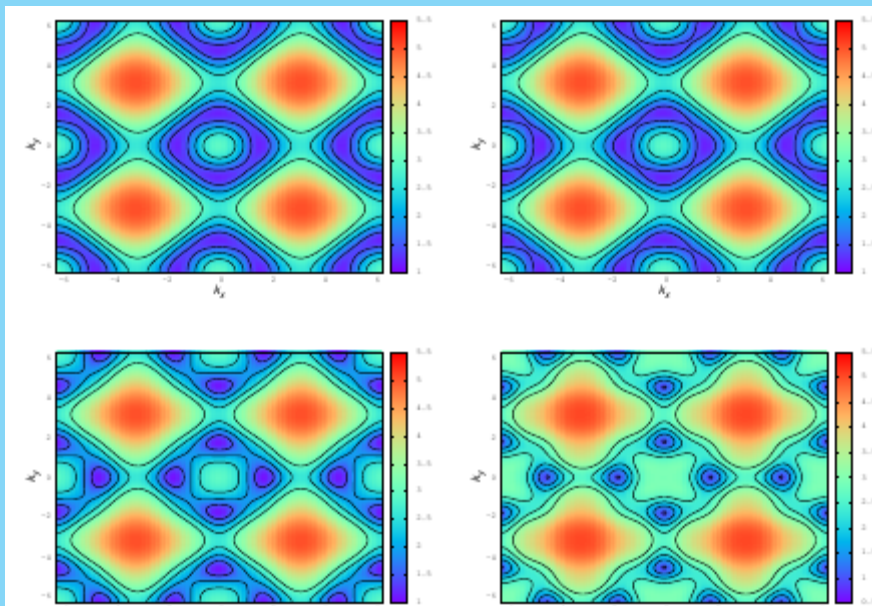


**Figure 2:** The dispersion relation for  $\Delta = 2.0$ ,  $B = 1.0$ ,  $B_2 = 0.20$ ,  $A_2 = 0.2$ ,  $B_3 = 0.04$  and four different values of  $A_3$ . (a)  $A_3 = 0.05$ , (b)  $A_3 = 0.10$ , (c)  $A_3 = 0.50$  and (d)  $A_3 = 1.00$ . The energies increase from blue to red

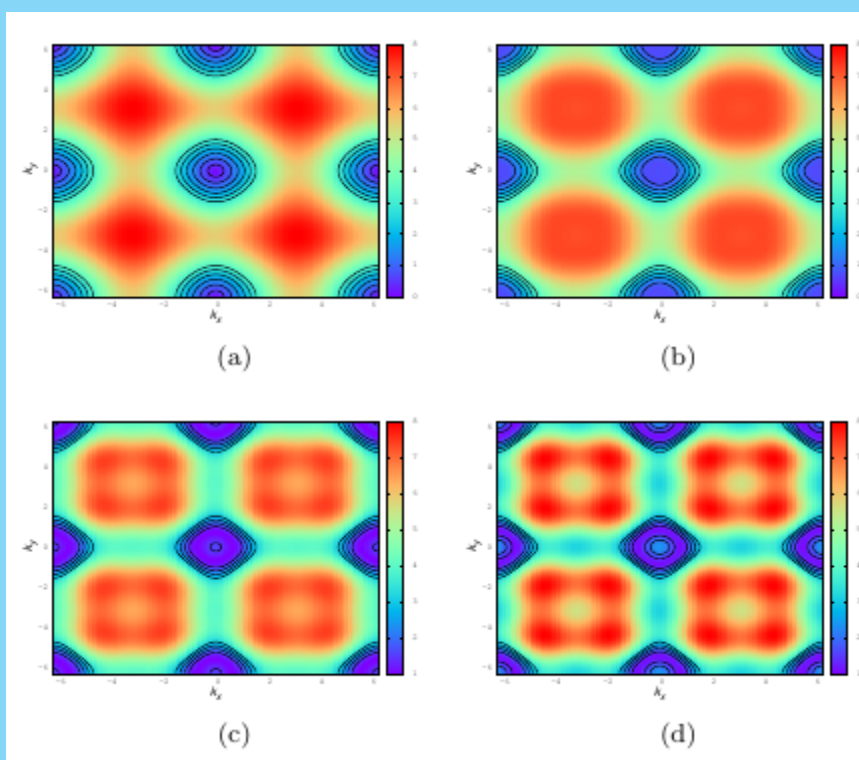


**Figure 3:** The dispersion relation for  $\Delta = 0.0$ ,  $B = 1.0$ ,  $A = 1.0$ ,  $A_2 = 0.20$ ,  $A_3 = 0.20$  and four different values of  $B_3$ . (a)  $B_3 = 0.00$ , (b)  $B_3 = 0.20$ , (c)  $B_3 = 0.40$  and (d)  $B_3 = 0.60$ . The energies increase from blue to red

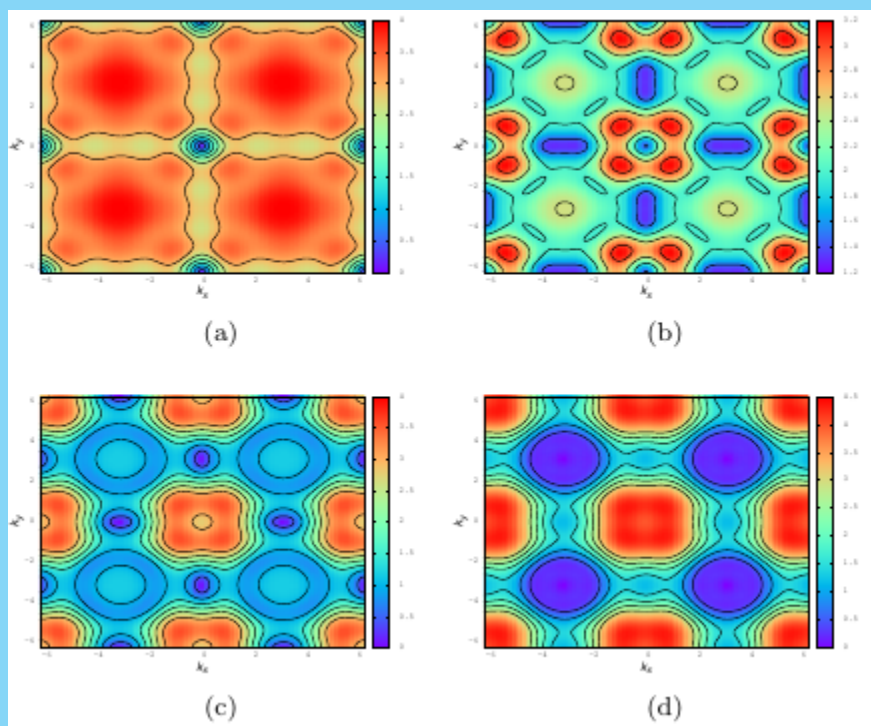


**Figure 4:** The dispersion relation for different values of  $\Delta$ , for  $A1 = 1.50$ ,  $B1 = 0.50$ ,  $A2 = 0.90$ ,  $A3 = 0.63$ , and  $B3 = 0.02$ . (a)  $\Delta = -0.48$ , (b)  $\Delta = 1.00$ , (c)  $\Delta = 2.32$  and (d)  $\Delta = 3.50$ . The energy increases from blue to red

## Conclusion

We have theoretically studied the effect of second and third neighbors on the topological insulator using a tight-binding model. It has been found that the energy band of the  $Z_2$  topological can change drastically depending on the hopping parameters of the second and third neighbors. The emergent singularities in the transition are important for the construction of superconductors with a better transition temperature. The effects of Lifshitz transition are important in different areas of physics.

## References

1. Lifshitz IM. Anomalies of electron characteristics of a metal in the high pressure region. *Sov. Phys. JETP*. 1960; 11:1130.
2. Volovik GE. Quantum phase transitions from topology in momentum space. *Springer Lecture Notes in Physics*. 2007; 718:3173.
3. Volovik GE. Topological Lifshitz transitions. *Fizika Nizkikh Temperatur*. 2017; 43:5767. arXiv:1606.08318.
4. Fu L, Kane C, Mele E. Topological Insulators in Three Dimensions. *Phys. Rev. Lett.* 2007; 98:106803.
5. Fu L, Kane CL. Topological Insulators with Inversion Symmetry. *Phys. Rev. B*. 2007; 76:045302.
6. Wu C, Bernevig BA, Zhang SC. Helical Liquid and the Edge of Quantum Spin Hall Systems. *Phys. Rev. Lett.* 2006; 96:106401.
7. Konig M, Wiedmann S, Brune C, Roth A, Buhmann H, Molenkamp LW, et al. Quantum Spin Hall Insulator State in HgTe Quantum Wells. *Science*. 2007; 318:766.
8. Hasan MZ, Kane CL. Colloquium: Topological insulators. *Rev. Mod. Phys.* 2010; 82:30453067.
9. Wrasse EO, Schmidt TM. Prediction of Two-Dimensional Topological Crystalline Insulator in PbSe Monolayer. *Nano Lett.* 2014; 14:5717.
10. Konig M, Buhmann H, Molenkamp LW, Hughes T, Liu CX, Qi XL, et al. The Quantum Spin Hall Effect: Theory and Experiment. *J. Phys. Soc. Jpn.* 2008; 77:031007.
11. Zhou B, Lu HZ, Chu RL, Shen SQ, Niu Q. Finite Size Effects on Helical Edge States in a Quantum Spin-Hall System. *Phys. Rev. Lett.* 2008; 101:246807.
12. Imura KI, Yamakage A, Mao S, Hotta A, Kuramoto Y. Zigzag Edge Modes in a  $Z_2$  Topological Insulator: Reentrance and Completely Flat Spectrum. *Phys. Rev. B*. 2010; 82:085118.
13. Mao S, Kuramoto Y, Imura KI, Yamakage A. Analytic Theory of Edge Modes in Topological Insulators. *J. Phys. Soc. Jpn.* 2010; 79:124709.
14. Mao S, Yamakage A, Kuramoto Y. Tight-binding model for topological insulators: Analysis of helical surface modes over the whole Brillouin zone. *Phys. Rev. B*. 2011; 84:115413.
15. Bernevig BA, Hughes TL, Zhang SC. Quantum Spin Hall Effect and Topological Phase Transition in HgTe Quantum Wells. *Science*. 2006; 314:1757.
16. Hsieh D, Xia Y, Wray L, Qian D, Pal A, Dil JH, et al. Observation of Unconventional Quantum Spin Textures in Topological Insulators. *Science*. 2009; 323:919.
17. Anilton de B. V. Filho, Raimundo N. Costa Filho. Topological insulators with second and third-neighbor couplings. *Phys. Lett. A*. 2017; 381:2123-2126.